"HAYNES" ALLOY NO. 188 AGING CHARACTERISTICS

R. B. Herchenroeder

Abstract

HAYNES alloy No. 188 is a cobalt-base solid solution strengthened alloy which has the strength characteristics of HAYNES alloy No. 25 and the oxidation characteristics of HASTELLOY alloy X through 2000°F.

The aging characteristics of HAYNES alloy No. 188 were studied by aging samples of the alloy in a gradient furnace (800 to 2000°F) for periods of 200, 500, 3400, and 6200 hours. Secondary constituents were identified by X-ray diffraction and the morphology of the phases present in aged samples were examined by microscopy.

A discussion of the precipitation reactions, phase morphology and post-aging ductility of the alloy is given.

R. B. Herchenroeder is a Physical Metallurgist with the Technology Laboratory of Materials Systems Division, Union Carbide Corporation, Kokomo, Indiana 46901.

Introduction

HAYNES alloy No. 188 was first introduced to industry during 1966. Since that time several large heats of the alloy have been produced and trial marketing initiated throughout the world.

Just what is HAYNES alloy No. 188?

It is an improved cobalt-base alloy which essentially incorporates the excellent oxidation resistance of HASTELLOY alloy X with the strength characteristics of HAYNES alloy No. 25 through 2000°F. In addition to this unique combination of properties, the alloy has high postaging ductility after being exposed in the intermediate temperature range of 1300 through 1800°F for prolonged periods of time.

The composition of the alloy is shown in Table I. At first inspection, the alloy's composition appears quite similar to that of HAYNES alloy No. 25 (L-605); however, there are several distinct differences. The alloy has a higher chromium content, a lower tungsten content and more than double the amount of nickel than HAYNES alloy No. 25 has. Further, the alloy contains a nominal 0.08 weight percent lanthanum which significantly enhances the oxidation resistance of the alloy.

HAYNES alloy No. 188 was developed because HASTELLOY alloy X, although possessing excellent oxidation resistance, often fell short of the strength needs at high temperature and because HAYNES alloy No. 25, while having the desirable strength levels, lacked oxidation resistance and tended to become embrittled after even short times of service in the intermediate temperature range of 1400 through 1800°F.

Since Jenkins first isolated the Laves phase commonly called Co_2W in HAYNES alloy No. 25, appreciable effort was devoted to the study of this cobalt-base alloy in attempts to eliminate the formation of the Laves phase or suppress its formation by people at Union Carbide Corporation, S. T. Wlodek, G. D. Sandrock, and others[1,2,3].

The use of electron vacancies or electron concentrations to predict the formation of intermetallics in nickel-base alloys is wide spread today; however, little use of this technique has been made for the predicting of phases in cobalt-base alloys. Work done by Professor Beck and his students at the University of Illinois link the formation of Laves phases to the electron concentrations of simple binary and ternary alloys[4] Woodyatt, Beattie, and Sims indicated that a Laves phase should not form at a electron vacancy concentration (N_V) of less than about 2.5[5]. In initial work, in developing HAYNES alloy No. 188, the concept of controlling the detrimental Laves phase in the new alloy was evaluated as shown in Table II. The N_V numbers form a nice correlation with the presence of the A_2B phase and the tendency of the aged sheet material to fracture during bending. Also, this work indicated that the N_V number at which the Laves phase would not form was about 2.66, but these calculations were made without consideration for such elements as chromium and tungsten being combined as carbides.

Paul Rainey, in evaluating the correlation of N_V numbers with the tendency of Co_2W to form, examined approximately twenty alloys and showed that there is a time relationship involved in the correlation[6]. This is shown in Figure 1. For short periods of time of approximately 25 hours, alloys with N_V numbers of less than about 2.5 remain ductile and little or no Laves phase was found in them. However, after 500 hours of aging at 1600°F the critical N_V number dropped to approximately 2.45.

Using this information the composition range of alloy No. 188 was established; the nominal composition as shown in Table I would yield an average electron vacancy concentration of 2.42.

The aging studies reported were conducted on sheet product from several larger heats of alloy No. 188.

Procedure

Samples of sheet approximately 5-1/2 inches wide by 11 inches long by 0.060 inch thick were placed in a gradient temperature furnace. These samples were aged for 200, 500, 2,884 hours, 3,360 hours or 6,244 hours. One of the sheet samples had thermocouples spot welded to it as shown in Figure 2 so that a relatively close monitoring of temperature could be maintained throughout the aging period over the entire length of the temperature gradient. Samples of the various heats were then stacked as shown in Figure 3 with spacers between each sheet to allow circulation of air and to avoid possible adhesion between the samples during the aging period.

Some variation in temperature occurred, especially during the longer exposure times of 3,000 and 6,000 hours duration. These variations have been plotted and are shown in Figure 4. The greatest deviation from the specified temperature that will be mentioned was approximately ±25 degrees. The results obtained give a good indication of the aging behavior of HAYNES alloy No. 188 for prolonged times.

After aging, the sheet samples were sectioned at 100°F increments. Part of the sheet sample was used for bend tests, part for metallographic examination, and part for extraction of microconstituents.

The samples were bent about a 2t radius on the rig shown in Figure 5. A typical specimen is shown in Figure 6 and would be approximately 1/4 inch wide, 1 inch long and about 0.063 inch thick.

A calculated relationship between the measured bend angle and tensile elongation is shown in Figure 7. Thus, a sample with a bend angle of 180 degrees without fracture would be expected to have 25 percent or greater tensile elongation; a sample with a measured bend angle of about 30 degrees would be expected to have a tensile elongation of approximately 4 percent.

Discussion

Aging, 200-500 Hours

The data in Figure 8 represents a single heat of HAYNES alloy No. 188, Heat No. 8188-6-106 which was used for each of the aging experiments. Unless otherwise noted the information presented in this paper will have been gathered from material from this heat.

After aging for 200 hours throughout the temperature range of 900 through 1800°F all of the samples passed the bend test by bending 180 degrees. After aging 500 hours throughout the temperature range all of the samples passed except those at 1600°F, where the average bend angle obtained was approximately 130 degrees.

Table III lists the microconstituents found in the alloy after these aging cycles. Immediately obvious is the absence of the Laves phase A_2B which would be present in appreciable amounts in HAYNES alloy No. 25, even with the lower silicon content material currently being produced. The ductility loss noted in Figure 8 is attributed to the precipitation of secondary M_6C and $M_{23}C_6$. Microprobe traces on the samples have shown that there is a lanthanum rich compound which is labeled in this table as La_xB_y phase; however, it has not been identified crystallographically by X-ray diffraction. The M_6C precipitates as low as 1600°F.

Figure 9 represents the annealed structure of alloy No. 188. The matrix is face-centered cubic and it has a random distribution of M_6C present. The lanthanum rich phase etches rather dark and is associated with some of the M_6C. The structure of the sample aged 200 hours at 1800°F is shown in Figure 10. There is the random distribution of both the primary and secondary M_6C and the M_6C precipitation along the grain boundaries. Randomly scattered in isolated areas are acicular particles which may be small particles of a Laves A_2B type phase; however, again this phase was not detected by X-ray diffraction.

The structure of the alloy after 500 hours at 1800°F is shown in Figure 11 and is quite similar to the alloy after 200 hours exposure.

After exposure for 200 hours at 1600°F the structure, Figure 12, of the alloy differs somewhat from the 1800°F structure, the matrix precipitation is much finer as is the precipitation along the grain boundaries. There seems to be preferential precipitation of the M_6C and $M_{23}C_6$ on the twin planes and grain boundaries as would be expected.

Figure 13 is a higher magnification of the structure of the sample aged for 200 hours at 1600°F. It appears that the precipitate along the grain boundaries are discreet particles in this micrograph while the particles forming along the twins are in a solid sheath.

Little change in the structure of the sample aged an additional 300 hours at 1600°F, Figure 14, was noted.

At twice the magnification, Figure 15, both a fine precipitate and distinct particles are resolved along the grain boundaries. Also, there are secondary particles noted adjacent to the primary M_6C, suggesting a decomposition of the M_6C and the formation of another phase, possible $M_{23}C_6$.

Precipitation of $M_{23}C_6$ during aging at 1400°F is much more pronounced both along the grain boundaries and along the twin planes. The size of these particles of precipitate are much smaller than that experienced at higher temperatures as would be expected. One could also note in Figure 16 that the primary M_6C scattered throughout the matrix seemed to have a halo of secondary precipitation around them, suggesting that the M_6C carbide decomposes as discussed earlier.

The increase in the amount of $M_{23}C_6$ during the period from 200-500 hours at 1400°F is negligible and it is difficult to distinguish between the structure of the sample aged 200 hours and that of the structure aged 500 hours (Figure 17).

Aging, 2,884-6,244 Hours

Microconstituents. Table IV tabulates the microconstituents found in four heats of alloy No. 188 after aging times of up to 6,244 hours throughout the temperature range of 800 through 2000°F.

Several general trends are apparent when this table is studied. First, in the intermediate temperature range of approximately 14 through 1600°F the M_6C carbide tends to disappear after prolonged aging. A unique and unexplained circumstance seems to exist with regard to the M6C carbide. For example, after 3,360 hours at 1600°F Heat No. 106 did not have any M_6C carbide present in the structure. However, after 6,244 hours exposure, apparently, the M_6C reappeared.

The same type of behavior was noted for Heats No. 121 and 122 although the phenomena occurred at a higher temperature; namely, the M_6C was absent at 1700°F after 3,360 hours but reappeared at 1700°F after 6,244 hours. This seems to violate the thermodynamic laws which indicate a system will seek the lowest energy state. If M_6C dissolves at 1600°F in 3,360 hours because the system seeks a low energy level, then there would seem to be no reason for M6C to reprecipitate during the next 3,000 hours of exposure time, unless it would be the location of the particles, i.e., matrix location versus grain boundaries.

The M_6C noted for temperatures 1700 through 2000°F comprised both primary M_6C and M_6C which precipitates during the aging time, as will be seen in subsequent photomicrographs of these pieces. Contrary to what was found for shorter times of 200 and 500 hours of aging, all of this M_6C had the same a_o of 11.03 angstroms.

$M_{23}C_6$ precipitates from 1100°F through 1800°F and possibly 1900°F in the system during 3,400 hours and this temperature range is expanded

down to 1000°F and up to definitely 1900°F after the 6,244 hours exposure. This seems to correlate well with the fact that after longer exposure times, the M_6C is dissolved at a lower temperature (1300°F). Thus, the M_6C particles are dissolved or are changed in stitu to $M_{23}C_6$.

Unfortunately, with the disappearance of the M_6C, the Laves phase A_2B appears -- first at the higher temperatures of 1800°F through 1400°F for the shorter period time of 3,360 hours, and then at lower temperatures for the longer exposure of more than 6,000 hours.

This is reasonable when one considers that the metal to carbon ratio of M_6C is 6 whereas the metal to carbon ratio in $M_{23}C_6$ is approximately 4. Thus, in any given system, as more of the M_6C dissolves and the carbon is combined as $M_{23}C_6$ more of the elements of the VI B group are available to form the undesirable A_2B phase.

Again, the unexpected occurred when a phase (A_2B) formed at a given temperature, in this case 1800°F at an intermediate time, dissolved again and disappeared after prolonged periods of time.

One should note that the Laves phase is found in alloy 188 in a relatively narrow temperature range and in some instances only very limited amounts of the phase are found. This correlates well with bend angle measurements and photomicrographs that we have of these samples.

In some of the samples exposed at the higher temperatures, Cr_2O_3 resulting from internal oxidation was extracted.

Also at the higher temperatures in some of the heats, an A_2B type phase was found which was different from the A_2B Laves phase discussed previously. Jenkins, in his work showed that the major interplannar d value distinguishing the Laves phase "Co_2W" from the $M_{23}C_6$ was 2.01. The X-ray diffraction pattern for the A_2B type noted here has the line at 2.01, but it does not have a diffraction line at 1.97. The line at 1.97 is needed in the normal A_2B pattern and in the $M_{23}C_6$ pattern. This particular phase does not seem to be influential with regard to the post-aging ductility of alloy No. 188.

Bend Ductility. Figure 18 shows the comparative bend ductility of two heats of alloy No. 188 and one heat of HAYNES alloy No. 25 which were simultaneously aged in the gradient furnace.

Alloy No. 188 does lose ductility in the intermediate temperature range, however, the temperature spread and the degree to which ductility is lost is markedly less than that for the alloy No. 25. (This incidentally was a heat of low silicon content, 0.18 w/o.) In the temperature range of 1200-1700°F for 3,360 hours, alloy No. 25 had a bend angle of approximately 10 degrees which converts to a calculated tensile ductility of about 1 to 2 percent (see Figure 7). Alloy No. 188, by contrast has a minimum bend ductility after 6,244 hours -- double the time -- of approximately 30 degrees which corresponds to a tensile elongation of approximately 4 percent. Ergo, HAYNES alloy No. 188 has a minimum ductility four times as great as that of alloy No. 25, even though exposed approximately twice as long.

The temperature range for embrittlement of HAYNES alloy No, 25 extends from 1200 to 1800°F for aging periods of 3,360 hours, whereas, for alloy No. 188, the minimum ductility span is only 200°F for the case of Heat No. 8188-6-106, and for Heat No. 121 the extent of minimum ductility is 400 degrees.

The graphs suggest that the samples overaged. Ductility was lost in the higher temperature range in both instances; as aging time progressed, the minimum ductility span moved towards lower temperatures.

Another factor of note is the temperature at which the different alloy 188 heats began to lose significant ductility. For Heat No. 8188-6-121, a significant loss of ductility was incurred at 1800°F after 3,360 hours; whereas, for Heat No. 8188-6-106, the first significant loss in ductility occurred at 1600°F after 3,360 hours.

This correlates well with the microconstituents found in the alloy and described previously in Table IV. Heat No. -121 had significant quantities of the Laves phase at 1800°F after 3,360 hours, Heat No. -106 did not have any A_2B at 1800°F and only a small amount at 1700°F.

The restoration of ductility also correlates well with the reappearance of the M_6C in the alloy after 6,244 hours and the disappearance of the Laves phase in samples aged at 1700°F, in the case of Heat No. -106, and at 1700 and 1800°F, in the case of Heat No. -121. Microstructures also correlate with this.

Microstructures. Figure 19 shows the structure of alloy No. 188 after 3,360 hours at 2000°F. Appreciable grain growth occurred, many of the M_6C particles dissolved, and others have coalesced into larger particles than those in the annealed piece. Some particles of Cr_2O_3 are also visible in the structure.

At 1900°F for 3,360 hours (Figure 20A), appreciable secondary precipitation of M_6C happened. This occurred randomly throughout the matrix and to some extent preferentially along the grain boundaries. This structure is quite similar to that of the alloy for shorter exposures and time.

Note in Figure 20B, after 6,244 hours at 1900°F, the M_6C coalesced appreciably accompanied by significant grain growth. There is some evidence of Cr_2O_3 resulting from internal oxidation.

At 1800°F, Figure 21A, there again was secondary precipitation of M_6C and the first evidence of the acicular phase normally associated with the A_2B Laves compound is seen. This Laves phase tends to appear along twin boundaries. After a longer period of time at 1800°F, Figure 21B, the M_6C distribution is approximately the same and the evidence of the presence of the A_2B phase is somewhat less.

For a comparison, Figure 22 is shown which represents Heat No. 8188-6-121. There is significantly more of the Laves phase present and

appreciably more evidence of internal oxidation indicated. This substantiates and correlates well with the bend data that we have for the alloy.

The structure in Figure 23 shows a random distribution of both M_6C and $M_{23}C_6$ type carbides and also an increased amount of the acicular phase of the A_2B type. Quite probably, the majority of the carbides are $M_{23}C_6$ with only small amounts of the primary M_6C remaining and very little secondary M_6C having been formed. Figure 23B, the structure of the alloy after 6,244 hours at 1700°F, shows the same general distribution of carbides as for the shorter time; however, there is a definite tendency towards coalescence of these carbides. Even though extraction and X-ray diffraction studies did not indicate as such, there does appear to be some of the acicular Laves A_2B phase present, again, distributed principally along the twins.

To correlate the difference in bend ductility and microconstituents found in two heats, Figure 24 is shown representing the structure of Heat -121 after 3,360 hours at 1700°F. Few of the larger particles, of what would be classified as primary M_6C, are present. The grain boundaries are essentially encompassed with the $M_{23}C_6$ and there is an appreciable amount of the A_2B type phase visible.

Figure 25A and B represent the structure of the alloy after 3,360 hours and 6,244 hours at 1600°F respectively. There is very little M_6C represented in Figure 25A, and the precipitates, in general, are fine and uniformly distributed throughout the structure. There is a sizable quantity of the acicular A_2B present. By contrast, the structure after the longer period of time, Figure 25B, shows that the acicular phase indeed overaged as indicated by the coalescence and growth of the particles. It is thought that the very fine precipitate along the grain boundaries is principally the $M_{23}C_6$.

To further illustrate the difference in the ductility behavior between the two heats being discussed, Figure 26A and B are shown for comparison with Figure 25A and B. For the shorter period of time, the Laves A_2B phase appears in long acicular particles oriented along the various crystallographic planes. The particles seem to be much coarser than those in the structure of Figure 25A. Figure 26B again indicates the tendency towards overaging and coalescent of the particles, but not to the extent for that of the Laves phase exhibited in Figure 25B.

A possible explanation of this variation in aging behavior could be a difference in thermal mechanical history. The annealed sample of Heat No. -121 had grossly larger grains and significantly fewer primary M_6C present than did the annealed structure of Heat No. -106. This suggests that, while the concentration of electron vacancies in the alloy determines the microconstituents which will form in the alloy at equilibrium, the thermo-mechanical history of the alloy will also be influential in determining the kinetics of the precipitation reaction and the morphology of the precipitating phases.

Figures 27A and B represent the structures of the alloy after aging at 1500°F. There was no M_6C found in the extractions for this structure indicating that the rounded particles shown have completely decomposed into some other phase quite probably $M_{23}C_6$ and/or the A_2B phase.

At 1400°F, the precipitation of the $M_{23}C_6$ along the grain boundaries is quite evident, Figure 28A. Little of the Laves phase is visible; however, a fine precipitate is evident along the twins and crystallographic planes of the alloy which could very well be the A_2B phase. Evidence to substantiate this is seen in Figure 28B, the structure of the alloy after 6,244 hours at 1400°F. The phase barely visible initially grew in size and became more evident. This also correlates well with the X-ray diffraction data which shows the tendency of the Laves phase to form at longer times at lower temperature.

Precipitation appears at 1200°F and at 1100°F with minor variations. The structure after 6,244 hours at 1100°F is shown in Figure 30A. X-ray diffraction data indicate that the only precipitate formed is $M_{23}C_6$. At 1000°F during 6,244 hours, Figure 30B, little precipitation occurred except along the grain boundaries, and this was $M_{23}C_6$. At 900°F, see Figure 31, the structure was essentially unchanged in 6,244 hours from the annealed condition shown earlier indicating the kinetics of the precipitation reaction, if any, are slow.

Figure 32 is a graphical representation of the hardness spread of the alloy after the longer aging periods, i.e., 3,360 hours and 6,244 hours. For the four heats examined, the annealed hardness ranged from approximately Rockwell A 57 through Rockwell A 62 which would correspond to about Rockwell B 93 through Rockwell C 23.

It was found that the lower hardness range was represented by Heat -121 and that the higher range of the hardness was represented by Heat-106 which further indicates that the starting materials have somewhat different thermo-mechanical histories even though this was not intended. Maximum hardness for the 3,360 hours was achieved by aging in the 1400 to 1500°F range as was the maximum hardness for the longer aging period of 6,244 hours. Above 1700°F, hardness of the aged samples at both aging times fell essentially in the same scatter band indicating that the materials were rapidly approaching equilibrium conditions. The final hardness of the material after prolonged aging at 1900 and 2000°F was always lower than the initial hardness. This would be expected from evidence of increased grain size and coalescence of the M_6C particles throughout the matrix.

What can be done to restore the ductility of alloy No. 188 after prolonged periods of aging and after such ductility is restored how long will the ductility persist when the samples are reaged?

Figure 33 represents the bend ductility of Heat No. 8188-7-0124 after being aged 2,884 hours across temperature range of 800 through 2000°F. The bend ductility behavior of this alloy is quite similar to that of Heat -106 discussed throughout this paper. Samples of this aged material were reannealed 15 minutes at 2150°F and then a portion of it bend tested. Note, all of the specimens bent 180 degrees without

fracture. Other samples that had been annealed after aging 2,884 hours were reaged an additional 100 hours at the temperatures indicated. These temperatures correspond to the temperatures at which the material had been aged previously. Again, after 100 hours at temperature, the samples all bent 180 degrees without fracture. After aging 500 hours at the indicated temperatures, all samples from 1100 through 1500°F passed the bend test; however, samples aged at 1600 and 1700°F did fracture.

Thus, it is shown that significant ductility can be restored to alloy No. 188 after prolonged aging by reannealing at 2150°F and that this restored ductility persists for extended periods of time.

Summary

The investigation has shown that a definite correlation exists between electron vacancy concentrations and the formation of detrimental Laves phase of the A_2B type. An improved alloy was designed using these criteria and it has been shown that the resulting alloy does have significantly better postaging ductility, both from the standpoint of degree of embrittlement and also from the standpoint of the temperature range in which the loss of ductility occurred, than does its predecessor HAYNES alloy No. 25. Further, it has been suggested that the kinetics of the precipitation reaction in the alloy can be associated to some extent with prior thermo-mechanical history.

The ductility of the alloy can be restored after prolonged aging by a short annealing or softening treatment at 2150°F and that this restored ductility will remain for extended periods of time when the material is re-exposed in the temperature range of 1100 through 1700°F.

Using the techniques described and the information gained from this study coupled with narrower chemistry ranges, there is no doubt that the postaging ductility of cobalt-base alloys of this type can be further enhanced and that a much better compromise between postaging ductility and high temperature strength and oxidation resistance can be achieved.

Acknowledgments

The writer is especially indebted to Messrs. W. E. Rutherford and J. Shutt for their assistance with the X-ray spectrography and metallography associated with this work, and in general to the personnel of the Technology Laboratory of Materials Systems Division, Union Carbide Corporation, for their assistance.

REFERENCES

1. E. E. Jenkins, Embrittlement of HAYNES Alloy No. 25 During Brazing. Project 817-1390, Haynes Stellite Company (Now Materials Systems Division, Union Carbide Corporation) Kokomo, Indiana, May 21, 1958.

2. S. T. Wlodek, Embrittlement of a Co-Cr-W (L-605) Alloy, Trans. ASM, Vol. 56, 1963, p. 287.

3. G. D. Sandrock et al., Effect of Silicon and Iron Content on Embrittlement of a Cobalt-Base Alloy (L-605), Cobalt No. 28, September 1965.

4. D. I. Bardos, K. P. Gupta, and Paul A. Beck, Ternary Laves Phases with Transition Elements and Silicon, Trans. of Metallurgical Soc. AIME, Vol. 221, Oct. 1961.

5. L. R. Woodyatt, H. J. Beattie, and C. T. Sims, Application of Periodic Group Effects and Phase Relationships to Stability of Nickel- and Cobalt-Base Superalloys and Stainless Steels, Paper at Fall AIME Meeting, Oct. 20, 1964.

6. P. E. Rainey, A Study of the Correlation of N_V Number with the Tendency of Co_2W to Form. Project 816-11500, Stellite Division, Union Carbide Corporation, Kokomo, Indiana, February 20, 1967.

TABLE I

HAYNES Developmental alloy No. 188

Chemical Composition, Weight Percent

Cr	Mn
22	0.75
W	Fe
14	1.5
Ni	La
22	0.08
C	Co
0.08	Bal
Si	
0.20	

TABLE II

N_V NUMBERS VERSUS ALLOY MICROCONSTITUENT A_2B

Heat No.	Angle of Bend, Degrees	N_V Number	X-ray Analysis A_2B
65-198	57	2.72	100*
65-197	67	2.72	100
65-199	72	2.72	100
65-197	85	2.72	100
65-198	98	2.72	100
65-230	93	2.68	100
65-217	61	2.66	60
65-217	158	2.66	40
65-222	180	2.66	
65-214	180	2.66	
65-228	180	2.65	
65-5	180	2.65	
66-8	180	2.65	
65-216	167	2.64	
65-221	180	2.64	
65-218	180	2.64	
64-81-1	180	2.61	
66-6	180	2.60	

All samples aged 200 hours at 1600°F

* Relative intensities of X-ray lines of X-ray diffraction pattern

TABLE III

HAYNES Developmental alloy No. 188 - METALLURGY

Solution Annealed	F.C.C. Matrix, Primary M_6C, La Rich Compound (La_xB_y), Associated with M_6C
Aged 1800°F	F.C.C. Matrix, Primary M_6C, La_xB_y, Secondary M_6C
Aged 1600°F	F.C.C. Matrix, Primary M_6C, La_xB_y, Secondary M_6C, $M_{23}C_6$
Aged 1400°F	F.C.C. Matrix, Primary M_6C, La_xB_y, Secondary $M_{23}C_6$
Aged 1200°F and Lower	Annealed Constituents

Samples Aged 200 and 500 Hours at Temperature

HAYNES Developmental alloy No. 188 MICRO CONSTITUE

AGING TEMPERATURE, °F	M_6C 3360 hrs.				M_6C 6244 hrs.				$M_{23}C_6$ 3360 hrs.				$M_{23}C_6$ 6244 hrs.				A_2B 3360 hrs.				A_2B 6244 hrs.				O 3360 hr		
HEAT →	A	B	C	D	A	B	C	D	A	B	C	D	A	B	C	D	A	B	C	D	A	B	C	D	A	B	C
2000	×	?	×	—	—	—				×	—		—				—										
1900	×	×	×	?	×		×			?	×		×	×	×		?										
1800	×	×	×	×	×	×	×		×		×	?	×	×	×		×										
1700	×			×	×	×	×		×		×	×	×	?	×		×	×	×			×					
1600				×	×				?	×	×	×	×	×	×		×	×	×	×	×	×	×				
1500									×	×	×	×	×	×	×		×	×	?	×	×	×	×				
1400			×						×	×	×	×	×	×	×		×	×		×	×	×	×				
1300	×		×	×			?		×	×	×	×	×	×	×			?		?	×	×	×				
1200	×		×	×	×	×	×		×	×	×	×	×	×	×		×				?	×					
1100	×		—	×	×	×	×			×	—	×	×	×	×			—									
1000	×	—	—	×	×	×	—		—	—			×	?	—		—	—				—					
900	×	—	—	×	×	×	—		—	—				—			—	—				—					
800	×	—	—	×	×	×	—		—	—				—			—	—				—					

A = Ht. 106 B = Ht. 121 C = Ht. 122 D = Ht. 124 (Aged only 2884

— = No Sample ? = Questionable presence.

Table IV

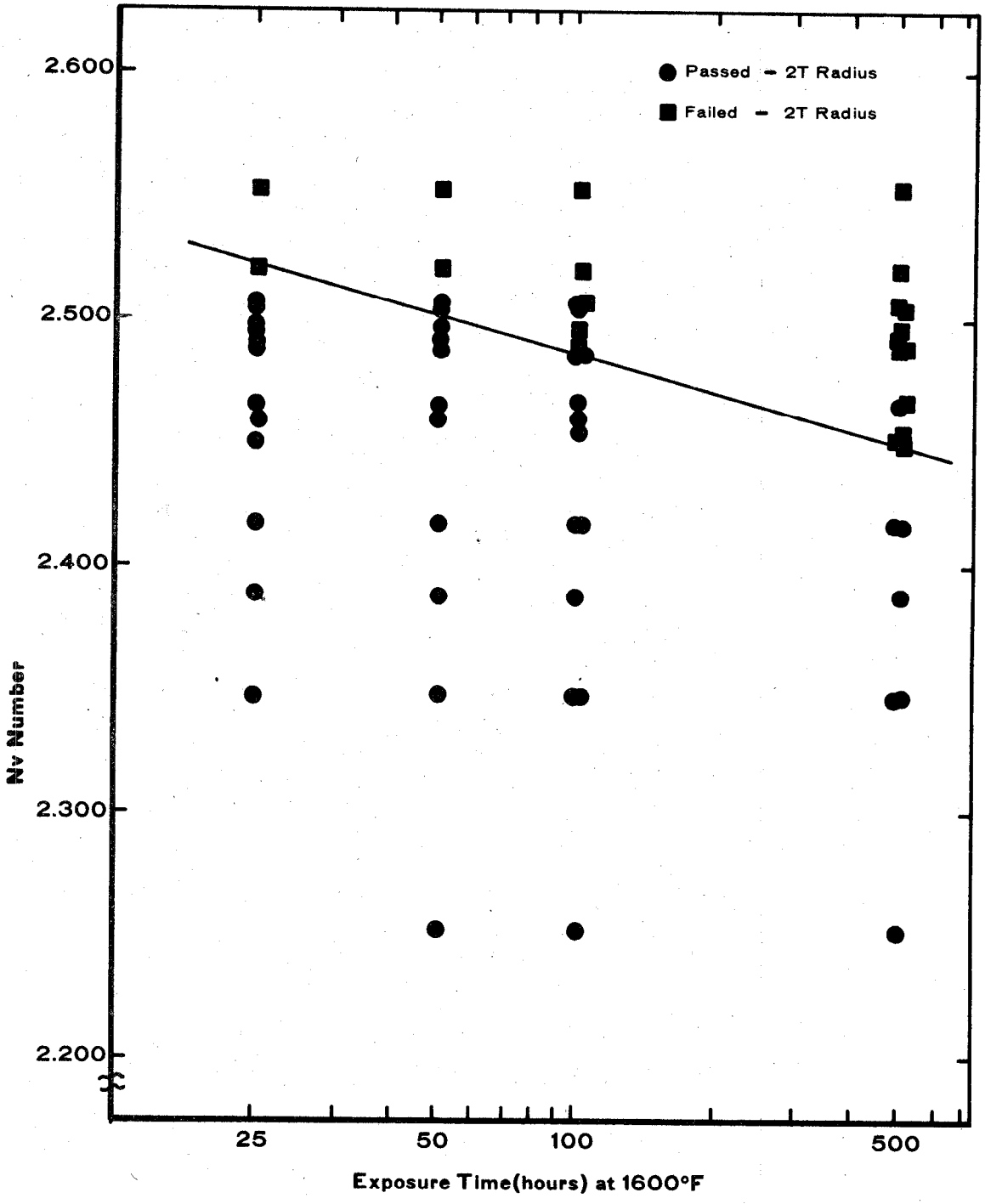

Figure 1 **Guided Bend Test Results**

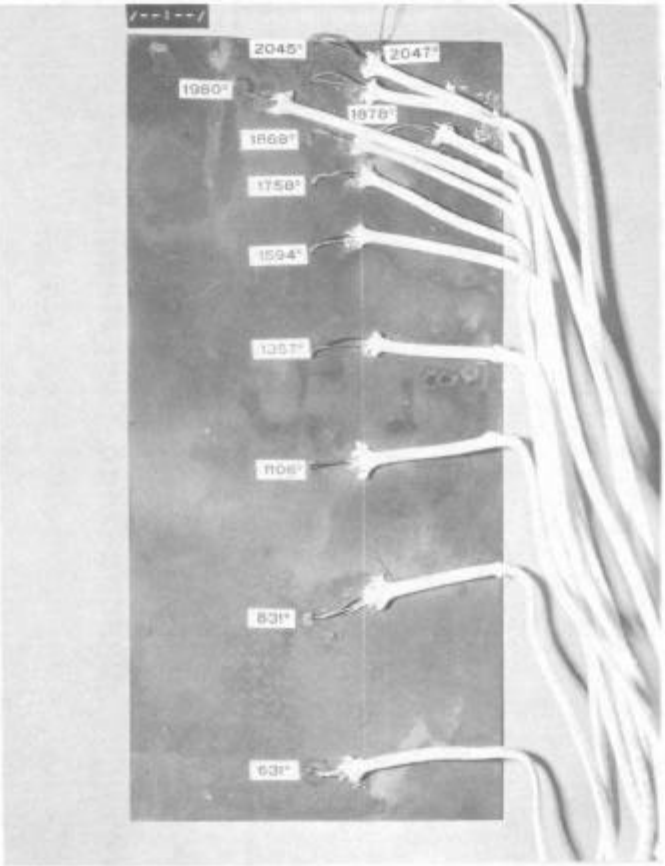

Figure 2: Thermocouple set up

Figure 3: Furnace pack

H-72217

H-7215

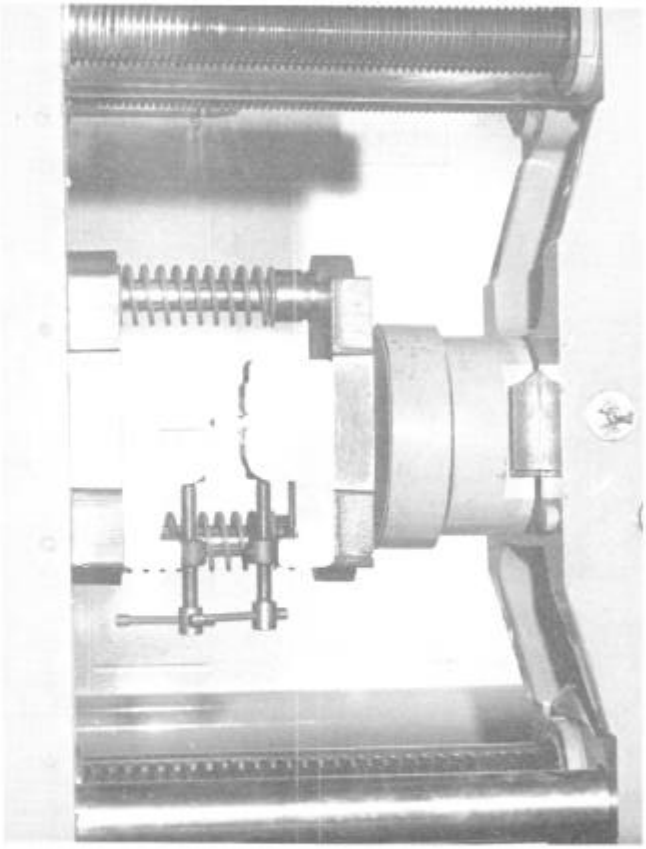

Figure 5: Bend test rig

Figure 6: Bend sample

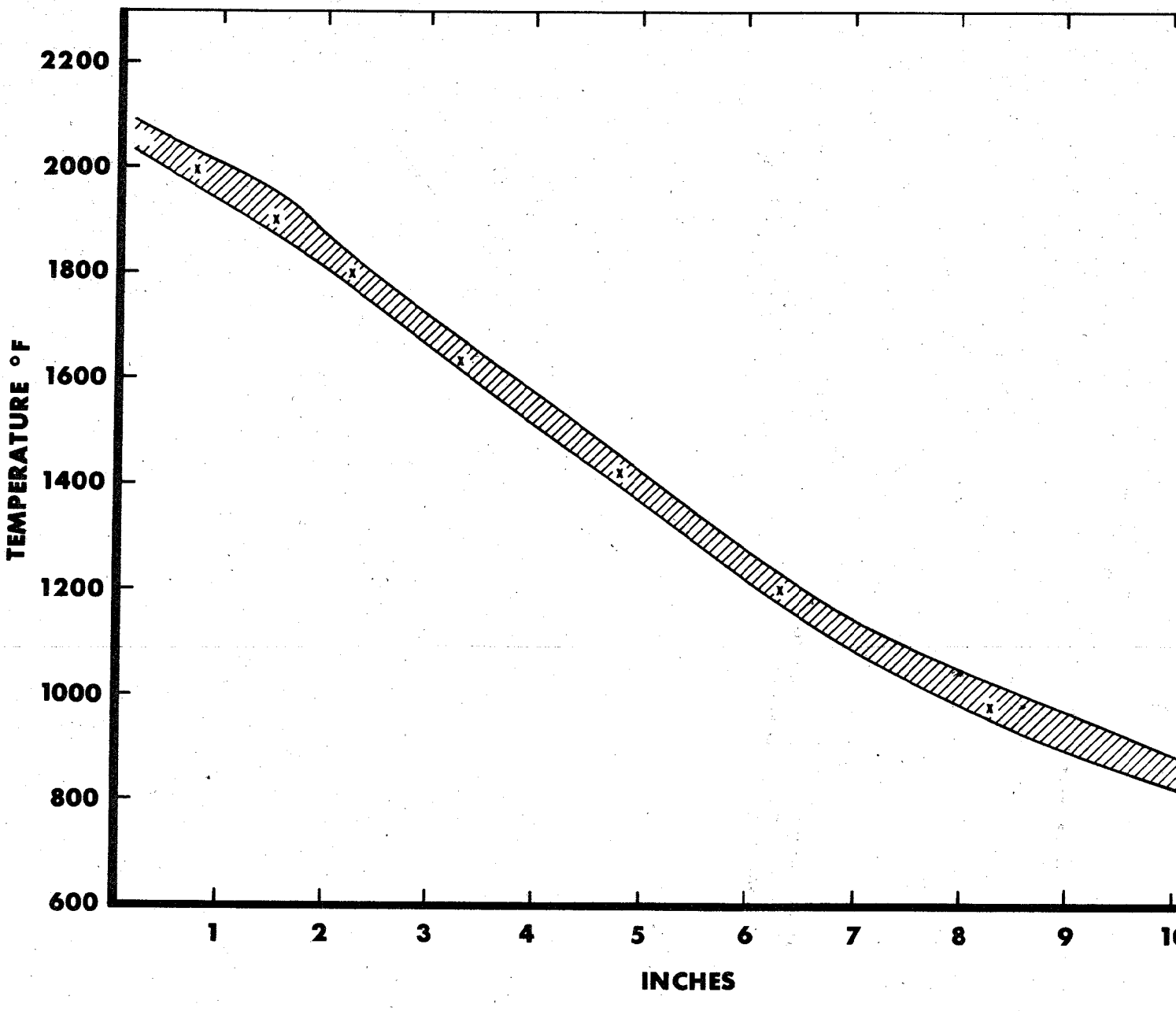

Figure 4 TEMPERATURE GRADIENT

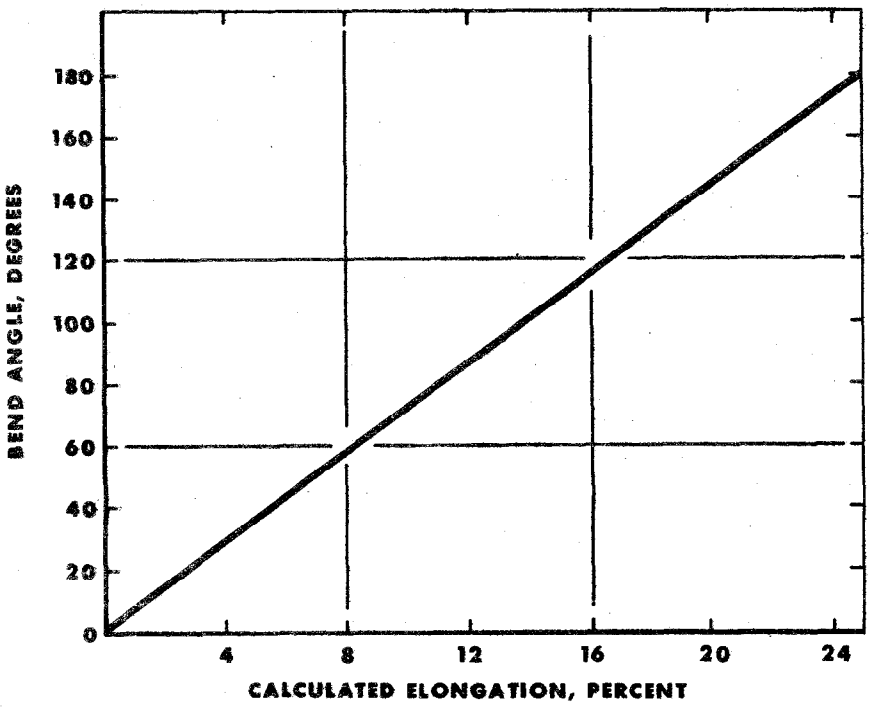

BEND DUCTILITY — CALCULATED ELONGATION

Figure 7

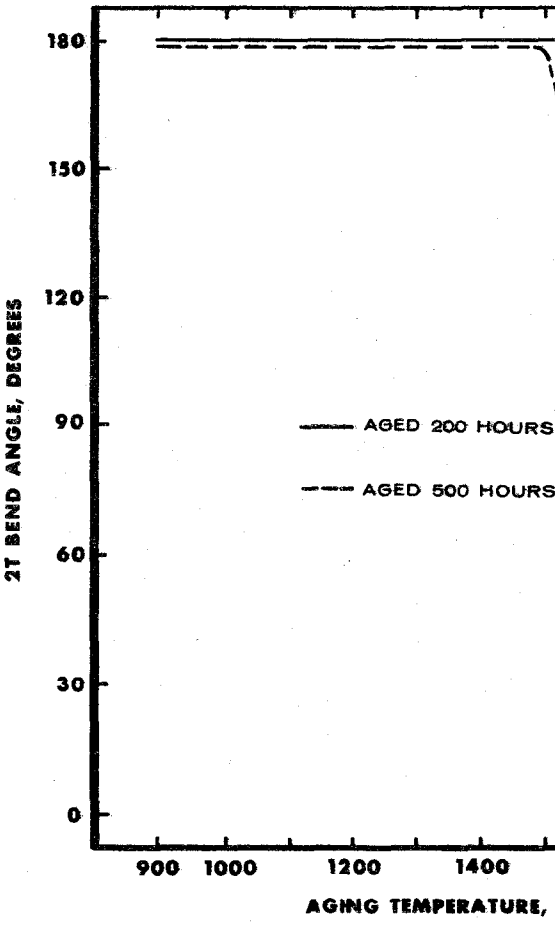

Figure 8 **HAYNES Developmental**

BEND DUCTILITY AG

Figure 9: Annealed Magnification: 500X

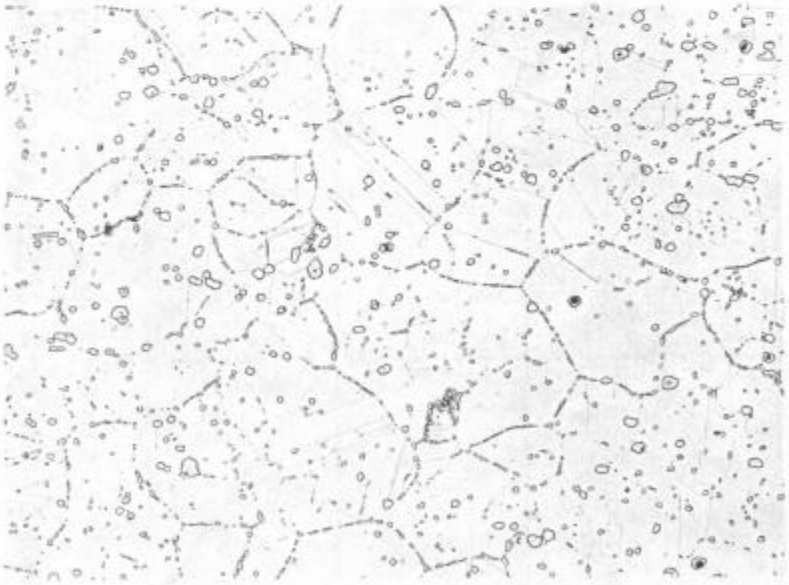

Figure 10: Aged 200 Hours at 1800°F Magnification: 500X

H-72159

H-72159

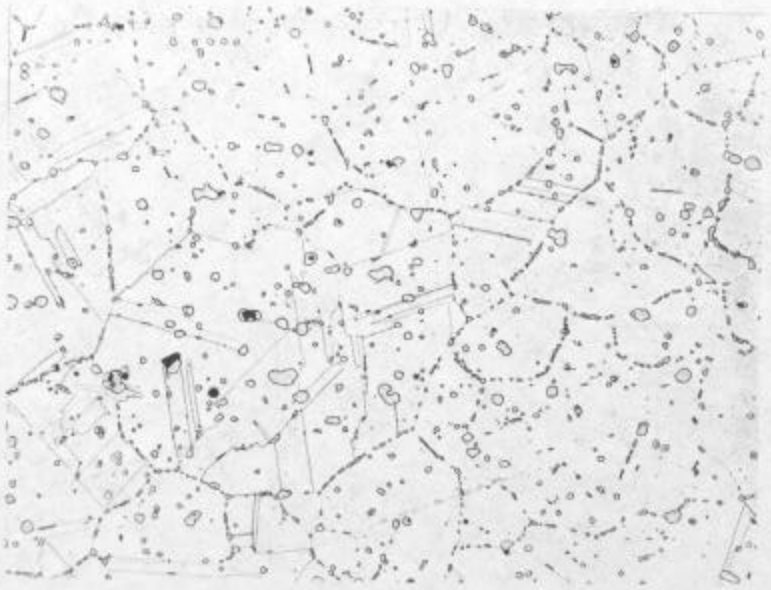

Figure 11: Aged 500 Hrs. at 1800°F Magnification: 500X

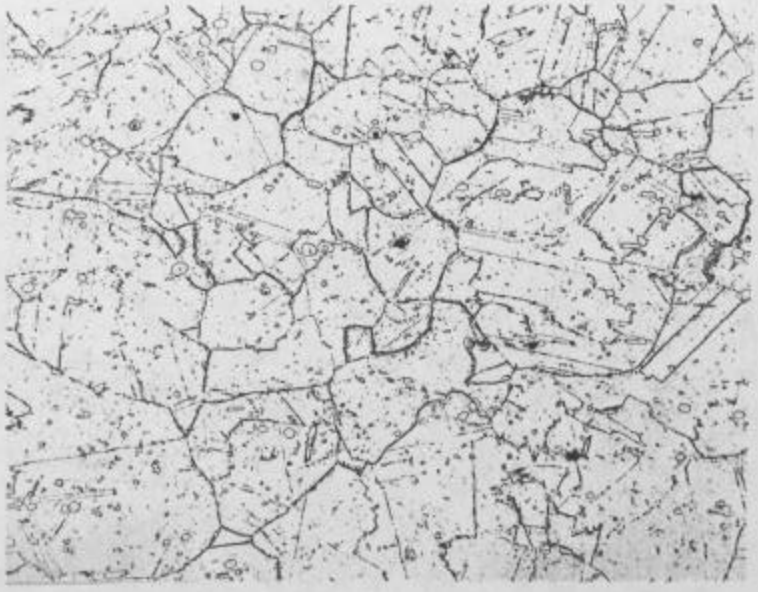

Figure 12: Aged 200 Hrs. at 1600°F Magnification: 500X

H-72160

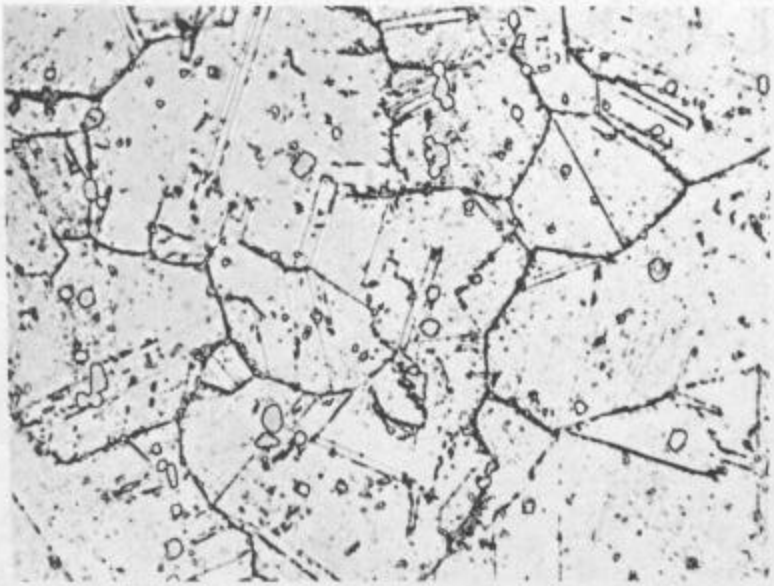

Figure 13: Aged 200 Hrs. at 1600°F Magnification: 1000X

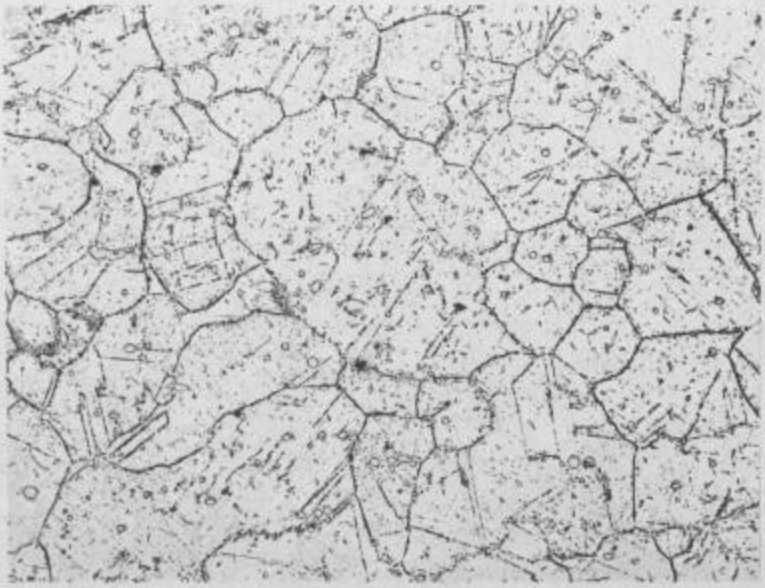

Figure 14: Aged 500 Hrs. at 1600°F Magnification: 500X

H-22161

H-72162

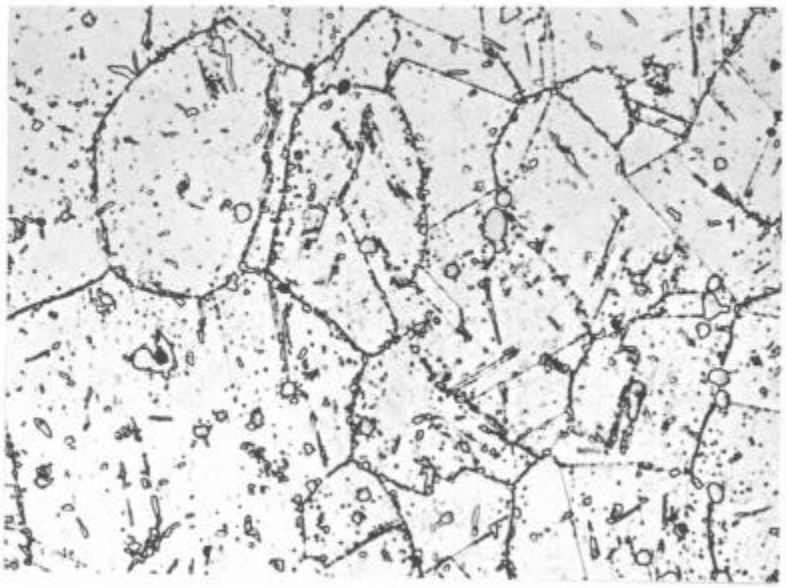

Figure 15: Aged 500 Hrs. at 1600°F Magnification: 1000X

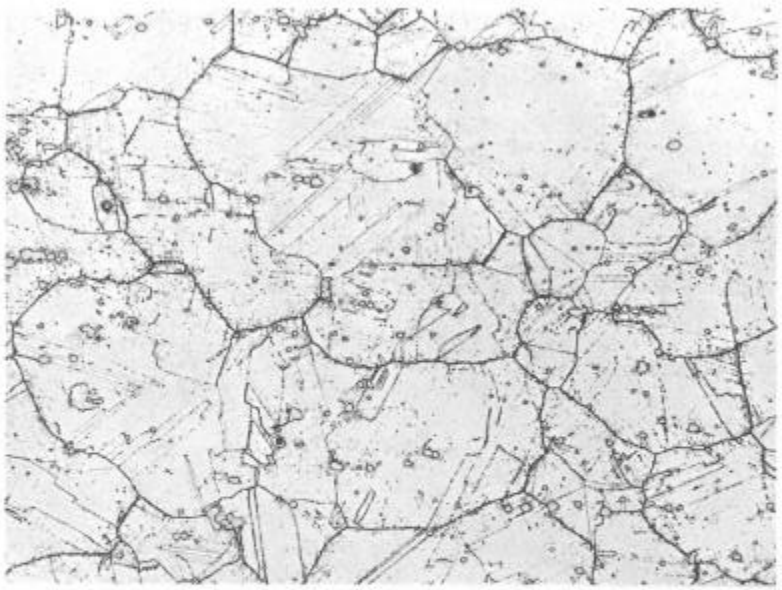

Figure 16: Aged 200 Hrs. at 1400°F Magnification: 500X

H-72162

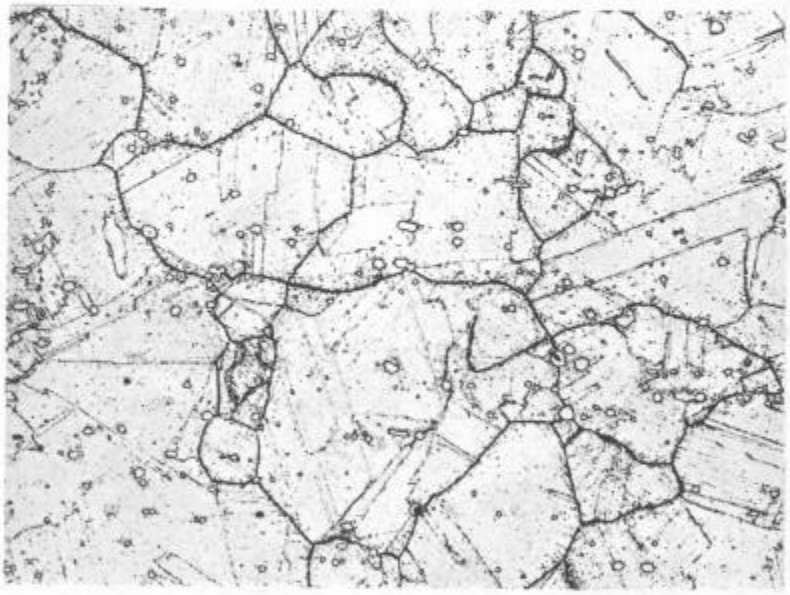

Figure 17: Aged 500 Hrs. at 1400°F Magnification: 500X

H-72163

H-72163

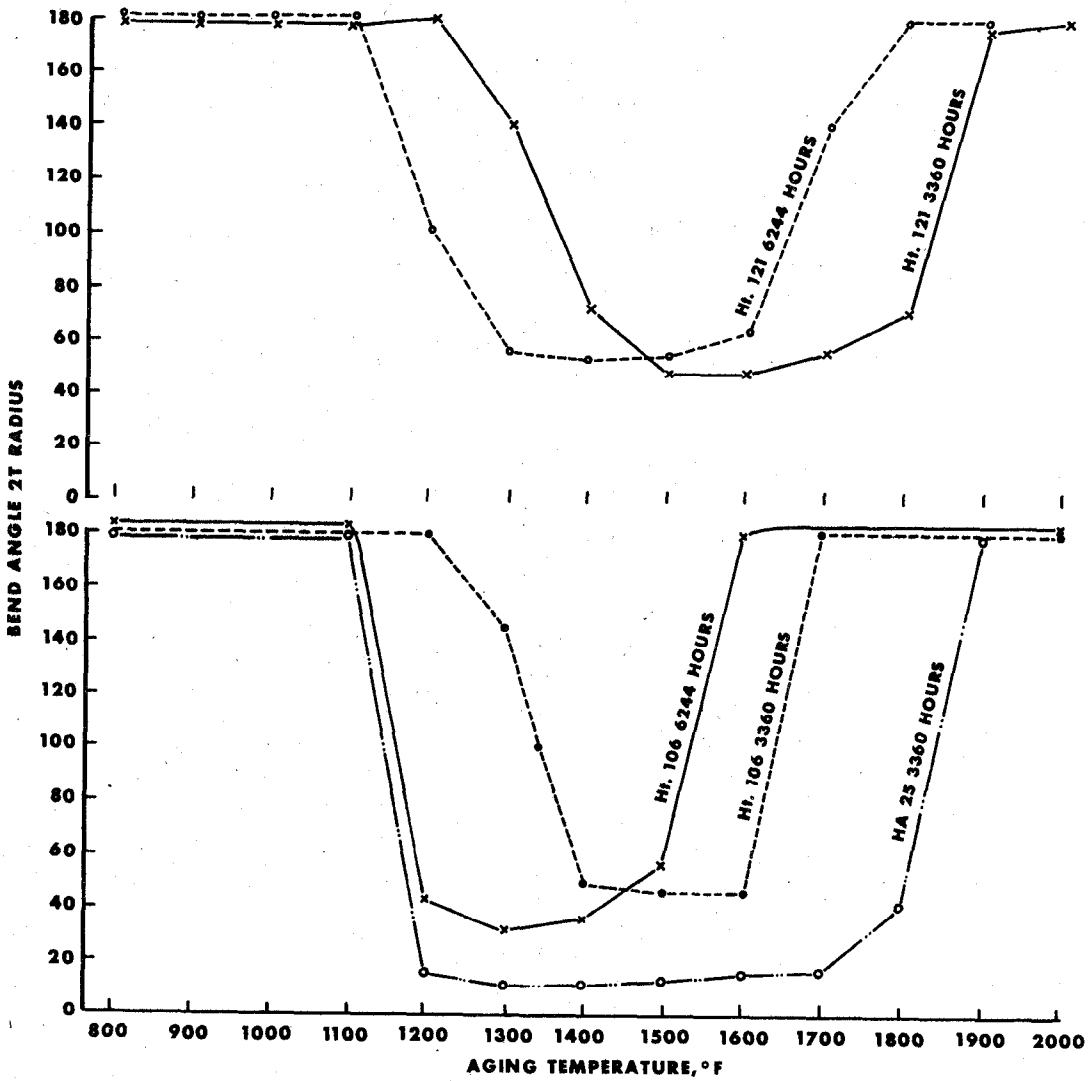

HAYNES Developmental alloy No. 188 BEND DUCTILITY

Figure 18

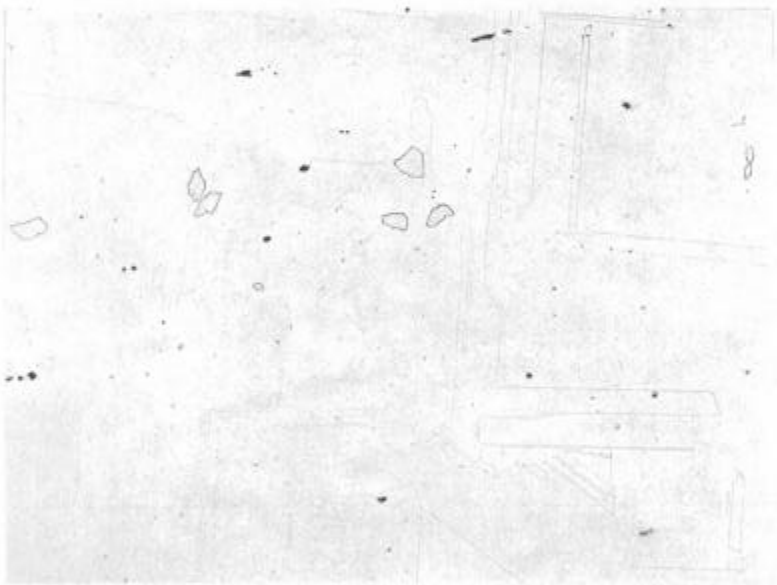

Figure 19: Aged 3360 Hrs. at 2000°F Magnification: 500X

H-72164

H-72164

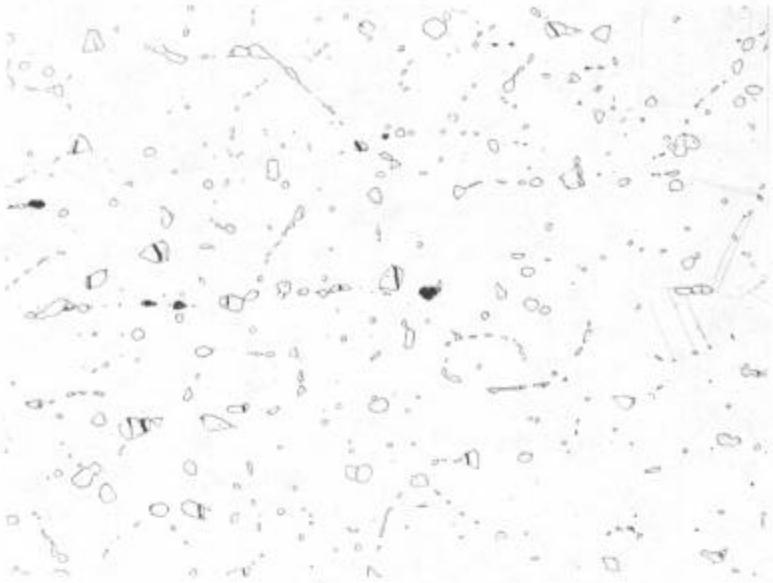

A - Aged 3360 Hrs. at 1900°F Magnification: 500X

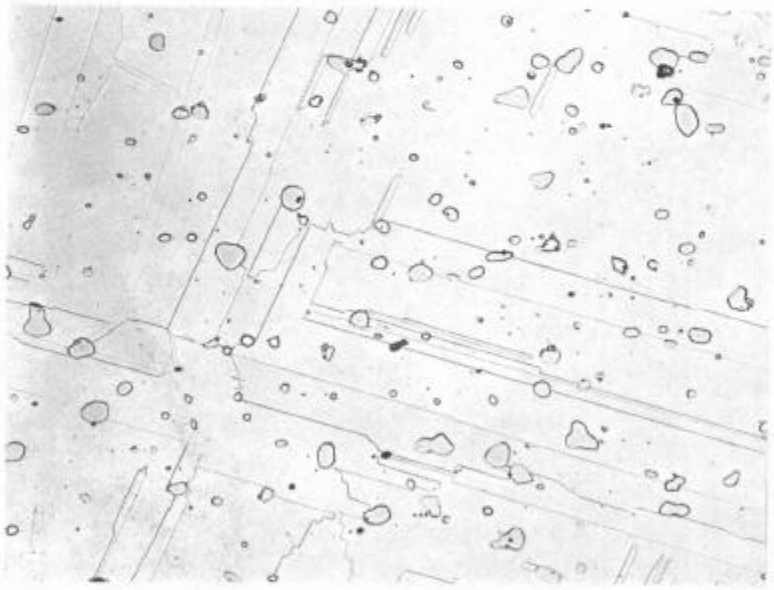

B - Aged 6244 Hrs. at 1900°F Magnification: 500X

Figure 20

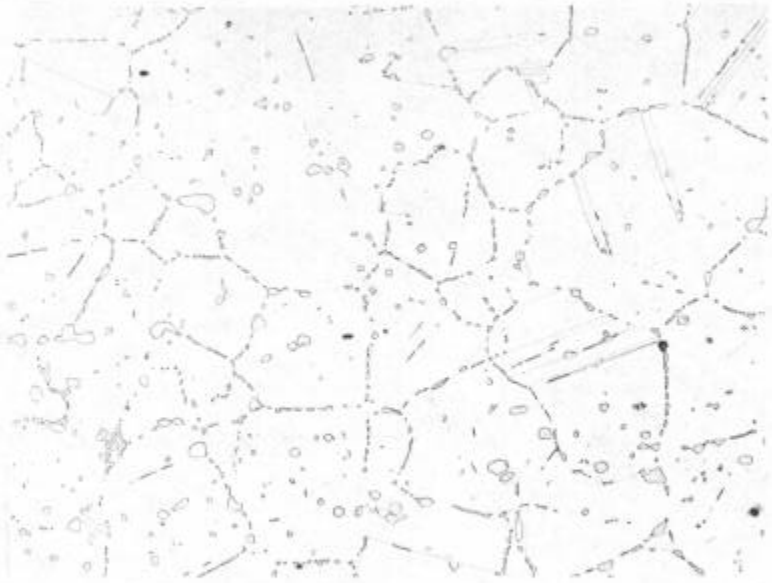

A - Aged 3360 Hrs. at 1800°F Magnification: 500X

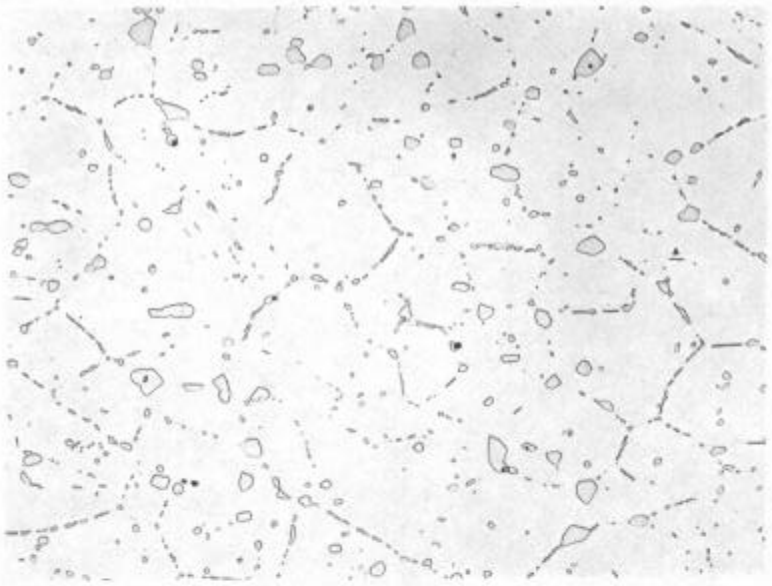

B - Aged 6244 Hrs. at 1800°F Magnification: 500X

Figure 21

H-72166

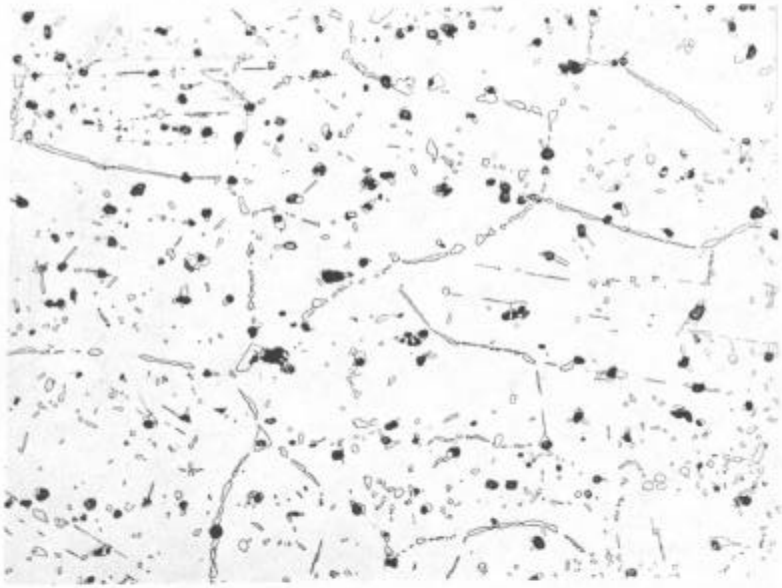

Figure 22: Ht. 121 Aged 3360 Hrs. at 1800°F Magnification: 500X

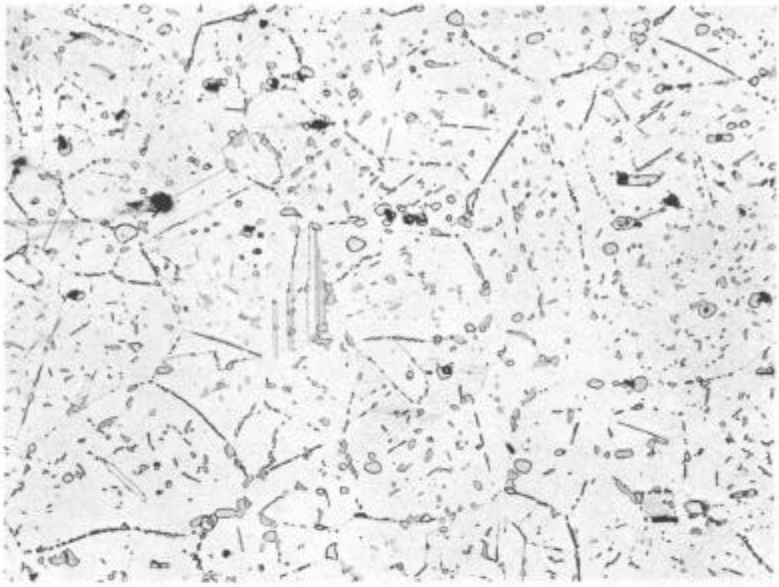

A - Aged 3360 Hrs. at 1700°F Magnification: 500X

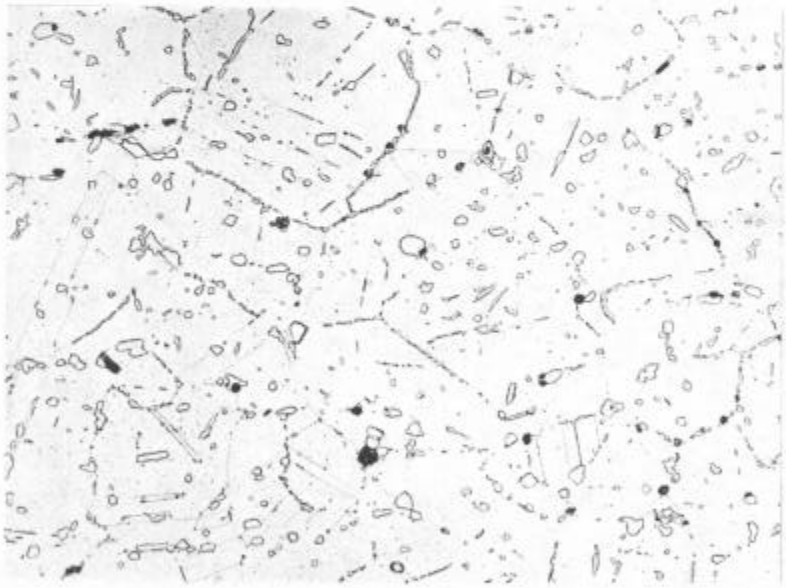

B - Aged 6244 Hrs. at 1700°F Magnification 500X

Figure 23

H-72168

Figure 24: Ht. 121 Aged 3360 Hrs. at 1700°F Magnification: 500X

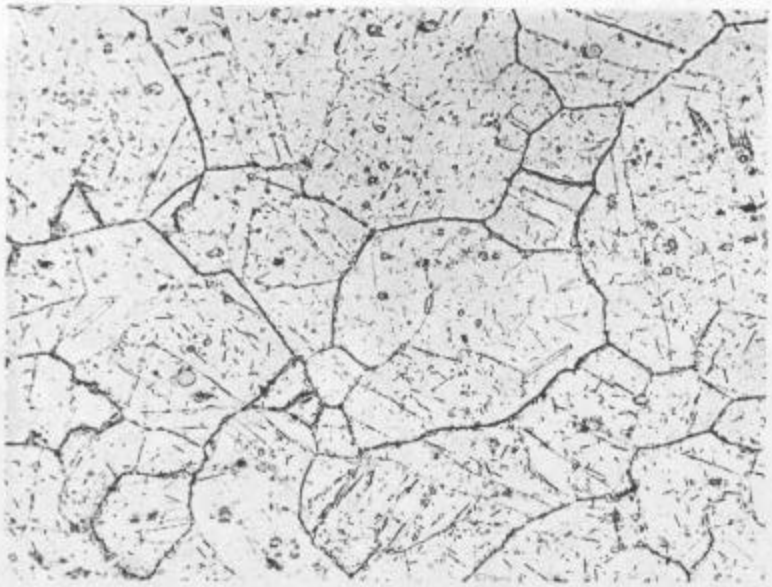

A - Aged 3360 Hrs. at 1600°F Magnification: 500X

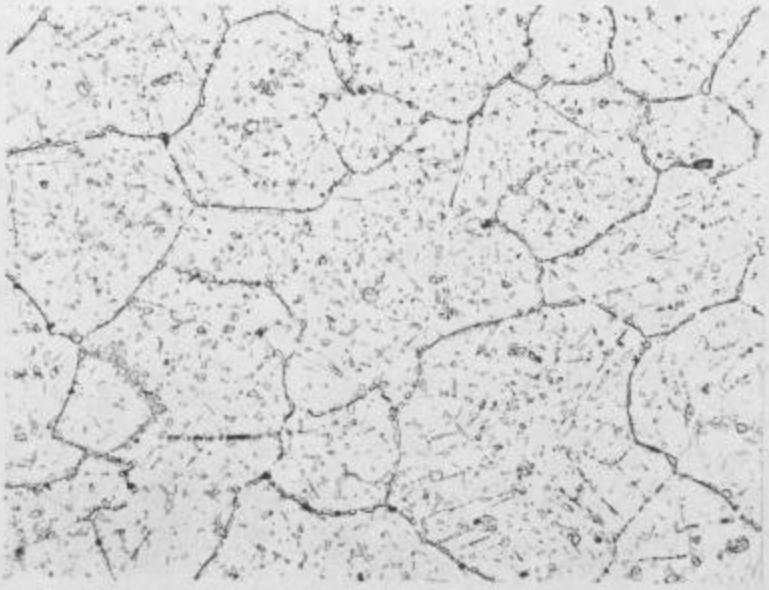

B - Aged 6244 Hrs. at 1600°F Magnification: 500X

Figure 25

H-72170

A - Ht. 121 Aged 3360 Hrs. at 1600°F Magnification: 500X

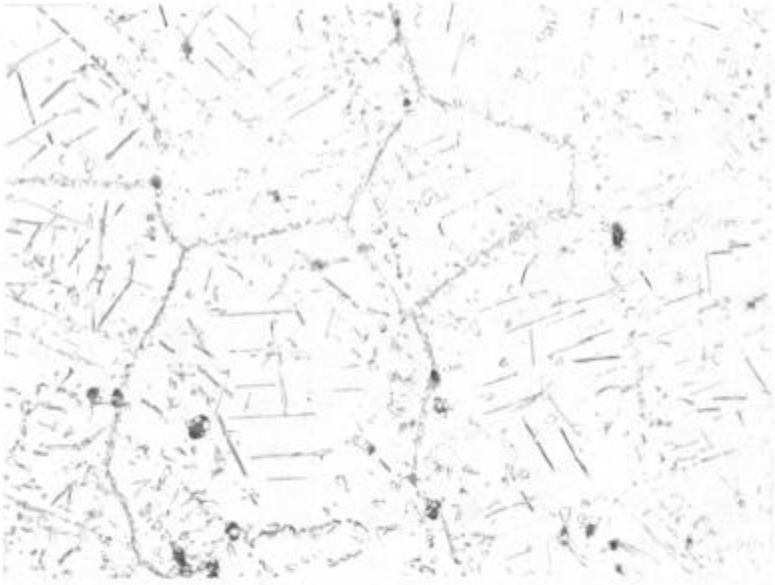

B - Ht. 121 Aged 6244 Hrs. at 1600°F Magnification: 500X

Figure 26

H-72171

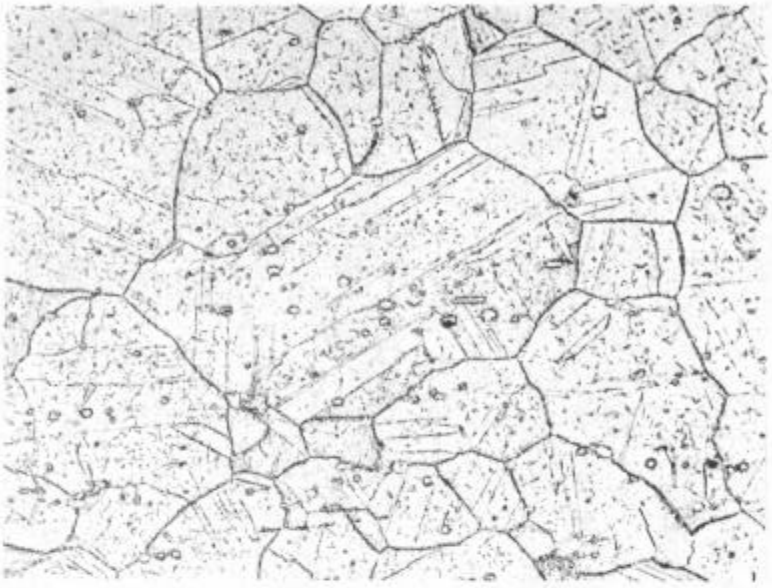

A - Aged 3360 Hrs. at 1500°F Magnification: 500X

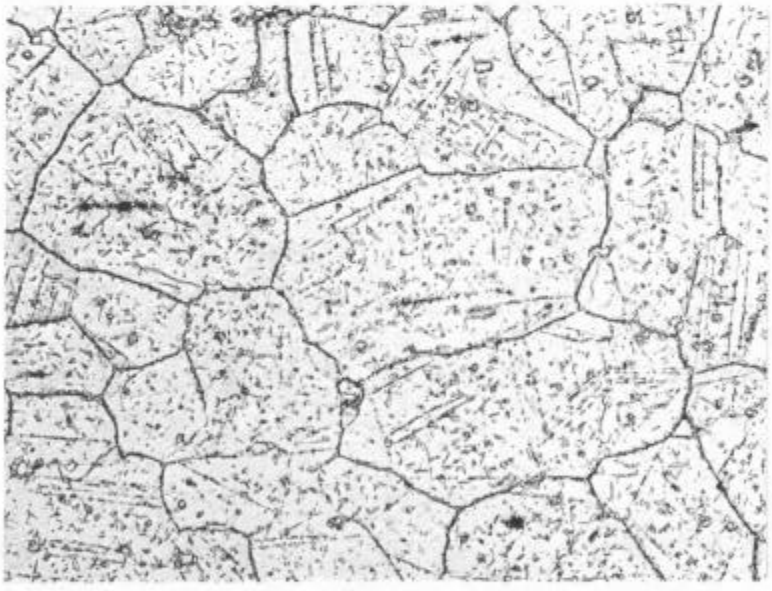

B - Aged 6244 Hrs. at 1500°F Magnification: 500X

Figure 27

H-72172

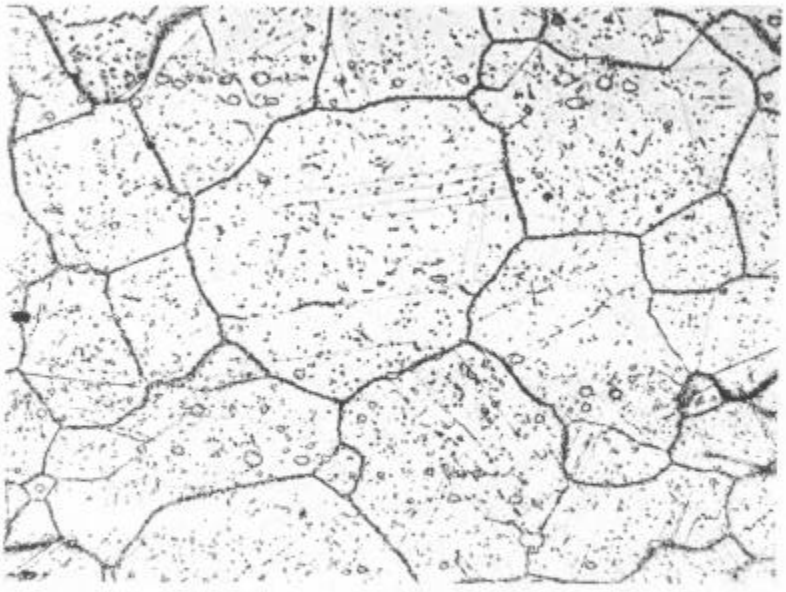

A - Aged 3360 Hrs. at 1400°F Magnification: 500X

B - Aged 6244 Hrs. at 1400°F Magnification: 500X

Figure 28

H-72173

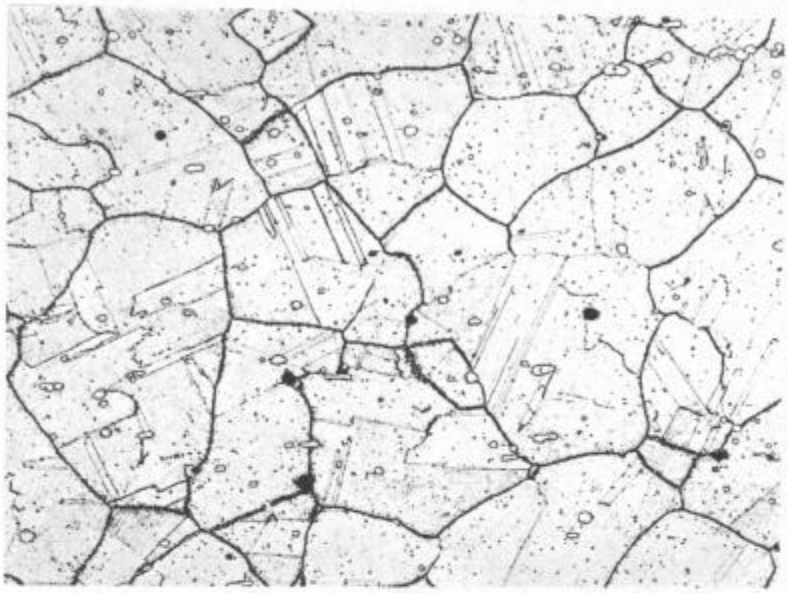

A - Aged 3360 Hrs. at 1300°F Magnification: 500X

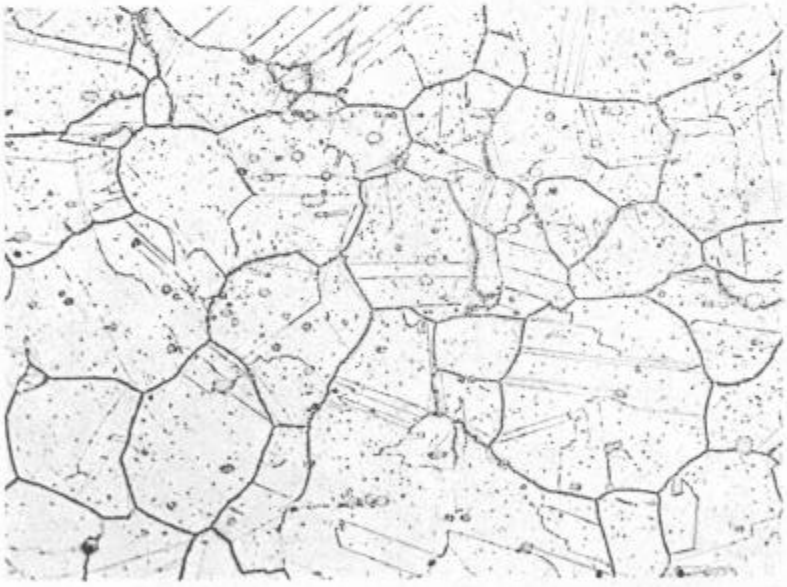

B - Aged 6244 Hrs. at 1300°F Magnification: 500X

Figure 29

H-72174

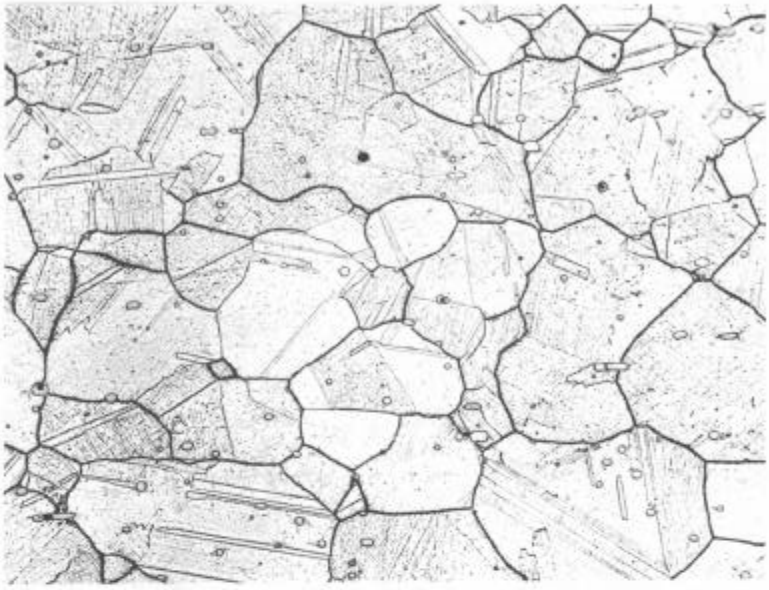

A - Aged 6244 Hrs. at 1100°F Magnification: 500X

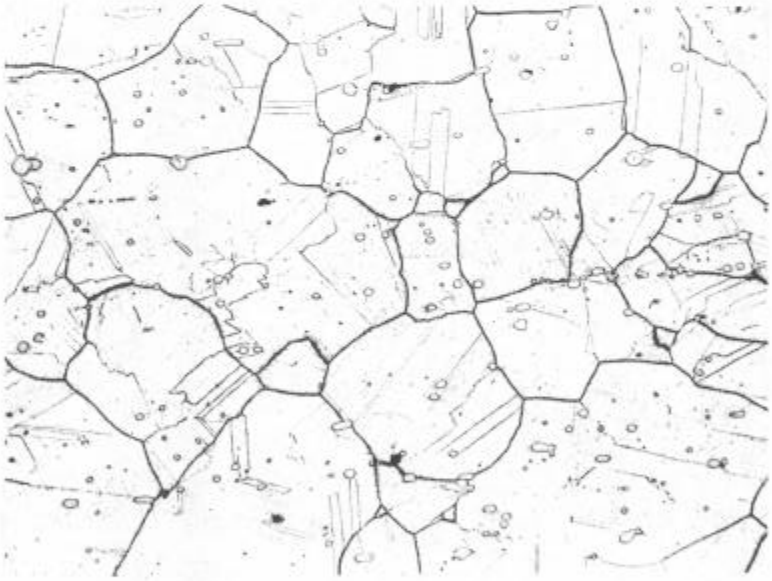

B - Aged 6244 Hrs. at 1000°F Magnification: 500X

Figure 30

H-72175

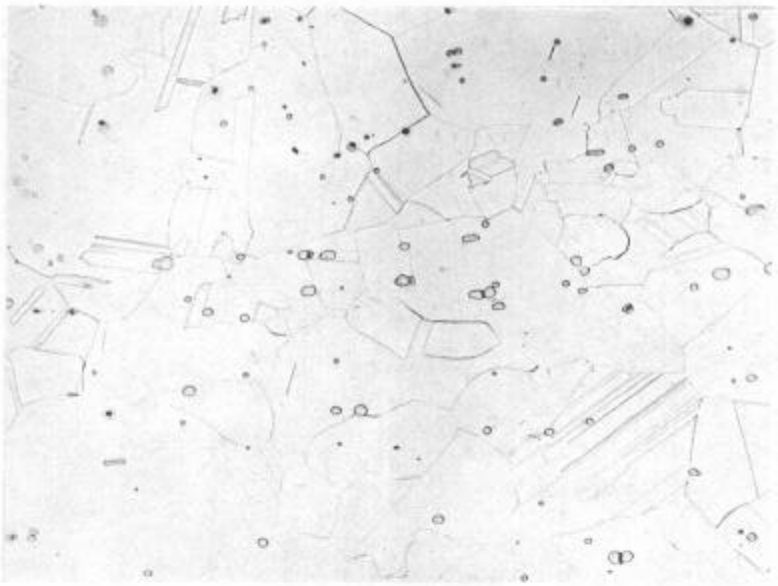

Figure 31: Aged 6244 Hrs. at 900°F Magnification: 500X

H-72176

H-72176

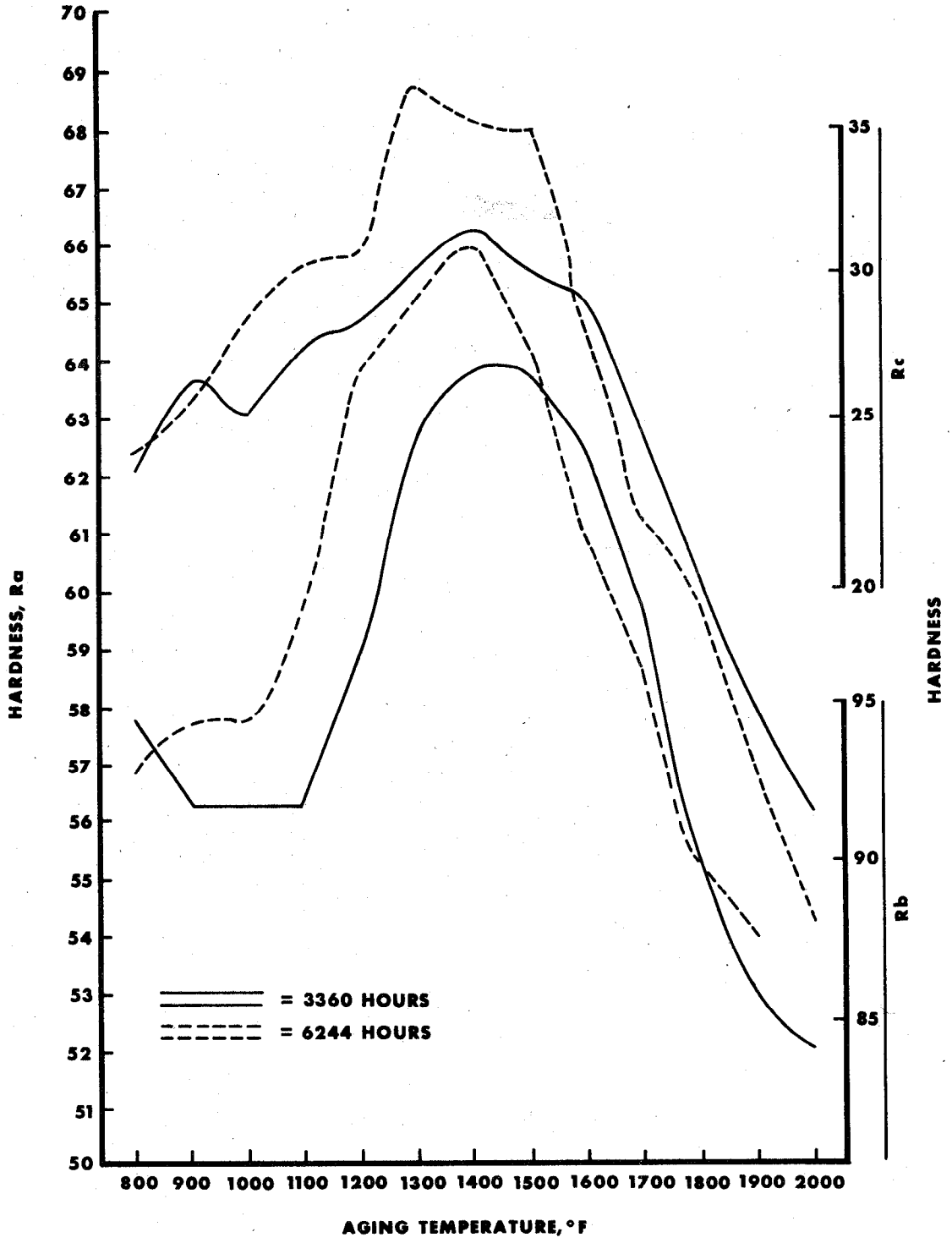

HAYNES Developmental alloy No. 188 AGED HARDNESS

Figure 32

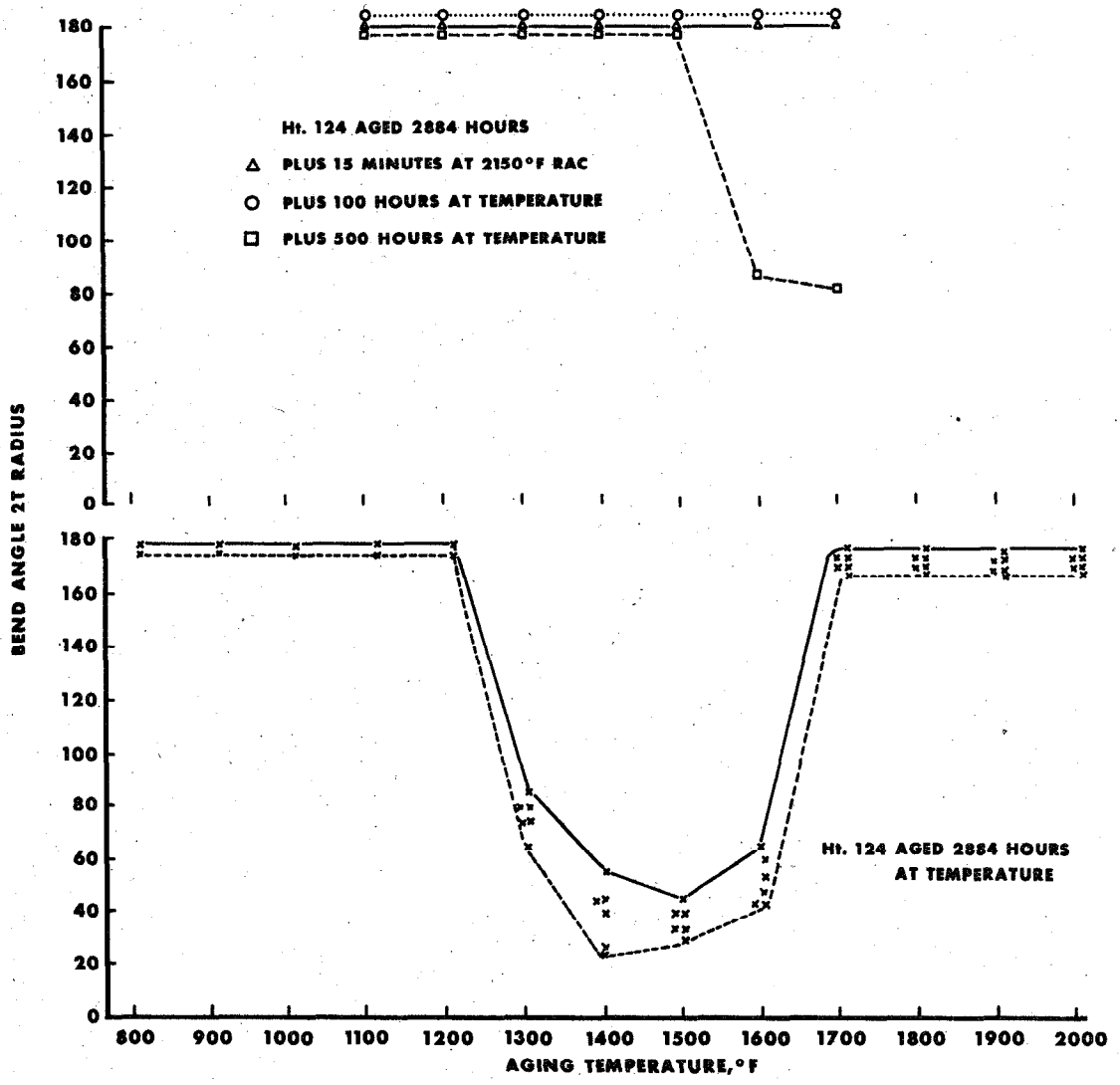

HAYNES Developmental alloy No. 188 BEND DUCTILITY

Figure 33